Pergamon

Geochimica et Cosmochimica Acta, Vol. 66, No. 12, pp. 2155–2165, 2002

0016-7037/02 $22.00 + .00

PII S0016-7037(02)00843-8

No mushy zones in the Earth's core

S. A. MORSE*

Department of Geosciences, University of Massachusetts, Amherst, MA 01003 USA

(*Received May* 29, 2001; *accepted in revised form January* 14, 2002)

Abstract—Mushy zones, assemblages of crystals and their pore-space liquids, have been invoked for both the upper and lower boundaries of the liquid outer core. The timescale of very slow accumulation compared with solidification at either of these interfaces militates against such zones, where instead hard ground should be expected to form by solidification at the interface. Such adcumulus growth involves isothermal, isocompositional solidification by successful exchange of evolving solute with fresh melt from an infinite reservoir. At both boundaries of the outer core, the removal of rejected material is significantly aided by compositional convection. The accumulation rates at the outer core boundaries are orders of magnitude slower than required for adcumulus growth, as calibrated both by field and experimental evidence in silicate melts. A conceptual phase diagram for the core–mantle boundary helps to visualize the relevant equilibria. Capture of core metal into the mantle has been suggested to occur via a mushy zone, to explain a high electrical conductivity there, as plausibly required by the secular behavior of the Earth's nutation. One conjecture is that the rejected light elements from the freezing of the inner core might be able to congregate as a porous flotation sediment at the top of the core. The idea of porosity in such a mushy zone must be rejected from experience with solidification of cumulates from magmas.

A high electrical conductivity might instead be caused by solution of core metal by mantle, followed by exsolution. The hottest part of the mantle lies in contact with the molten outer core, where the maximum solubility of Fe must occur in the major mantle phases. On leaving the core–mantle boundary, the mantle must cool and may exsolve metal on the metal–silicate solvus. If the iron-rich metal resides chiefly in the rheologically weaker metal oxide phase, which coats the deforming perovskite grains, it may furnish a short circuit for mantle conductivity in the basal mantle. At still cooler and higher levels, the mantle encounters more normal mantle redox conditions, and any exsolved Fe metal should oxidize to FeO in the metal oxide and perovskite phases, ceasing to be a conductor.

1. INTRODUCTION

The core is the Earth's largest magma chamber, sensu lato, and is hence subject to insights from igneous petrology as well as metallurgy. It combines the familiar behavior of molten metal with the less obvious but yet accessible behavior of silicate magma. An important insight from silicate magma chambers has been an appreciation of the importance of the boundary layers where cooling and solidification occur (e.g., Morse, 1986a; Marsh, 1996). The core freezes at the inner core boundary (ICB) and maybe at the top, and it certainly exports heat to the mantle at the Earth's largest thermal boundary layer (TBL). Conservative estimates of heat export from the core suggest that it amounts to 7 to 9% of the Earth's heat loss (Stacey, 1992; Hofmeister, 1999).

Persuasive seismological evidence suggests that the core melts the mantle at the D″ layer, locally forming giant silicate magma chambers that underlie and may feed hot spots (Garnero and Helmberger, 1996; Williams and Garnero, 1996). On the other hand, it has been proposed (Buffett et al., 2000, 2001) that the light elements rejected from the freezing ICB may collect beneath the mantle as porous flotation sediments that trap core metal and add it to the mantle. One need not tarry long in this wilderness to realize that the two ideas—melting and freezing of mantle material at the top of the core—are incompatible unless they occur at separate localities. The nature of the ICB, in particular the idea of constitutional supercooling, also requires review. Here, I address the action of material and heat at both boundaries of the outer core.

2. PHASE DIAGRAM FOR THE CORE

2.1. Constraints and Assumptions

To set the stage for discussion of events at the top and bottom of the outer core, some notion of the phase equilibrium relationships would be helpful. These relationships depend on our understanding of remotely sensed information from the core–mantle boundary (CMB) region, which I interpret as follows.

The CMB is defined at the junction of hot metal melt and silicate mantle, best identified by P-wave reflection from below. The lowest possible temperature at the CMB occurs where solid mantle notionally lies against core melt, where the mantle may chill the core to its liquidus. The highest CMB temperature is in principle unbounded at the coexistence of metal melt and silicate melt, but on grounds of stability, it cannot lie far from the equilibrium among metal melt, silicate melt, and mantle crystals. This boundary can be detected, in principle, by S-wave attenuation.

The temperature contrast across the seismic D″ layer is probably in the range 900 to 1300 K (Hofmeister, 1999), somewhat less than the range 1000 to 2000 K suggested by Williams (1998). The extreme limits of this bracket form a square wave between two potential temperatures: that of the core adiabat extended to the solid mantle, and that of the mantle

* (tm@geo.umass.edu).

adiabat extended to the molten core. Because of low viscosity and vigorous convection, the actual temperature at the top of the core is practically equal to the potential temperature. The associated TBL overlaps the D″ layer with an offset. The base of the TBL is effectively the top of the melt, whether metal or silicate, because the melt cannot sustain a sharp thermal gradient. Where a significant thickness of silicate melt exists, as it might in a giant magma chamber (Williams and Garnero, 1996), the base of the TBL lies within D″ at the base of the mushy zone that caps the silicate melt (Morse, 2000). The top of the TBL occurs where combined convection and conduction bring the ambient temperature to the mantle adiabat, a place that has no direct seismic signal. The TBL as described is taken to be the stable secular configuration, but it is plausibly subject to intermittent physical disturbances such as the escape of magma or the emplacement of slab material.

Of course, the mantle does not melt at a single point but at a cotectic among phases with variable Mg/Fe ratios. The phases considered here are aluminous Mg-Fe silicate perovskite, Ca-Al perovskite, and metal oxide (MO), essentially magnesiowüstite. The melting relations to be depicted are taken as the cotectic solidus at which the first mantle liquid is produced on melting (Morse, 2000).

Where the mantle chills the core, crystals of metal can be produced; whether these survive in time and space is moot, but on sinking, they constitute a cold finger, even if they simply melt with the absorption of latent heat. This action ultimately cools the ICB enough to cause crystallization. Where silicate magma occurs, the core loses heat most efficiently to the mantle by trading remote latent heat evolved at the ICB for latent heat consumed in the mantle. Hence, the place where the core loses heat fastest is where the mantle melts; but the place where the core is chilled is where the mantle is solid. These places are easily confused; think hot ocean ridge and cold slab, and there's the analogy.

A successful phase diagram must represent the principal observational constraints: core melt against solid mantle, against liquid mantle, and against liquid mantle with mantle crystals. The conceptual phase diagram offered in Figure 1 meets these criteria. The diagram represents only the high-temperature part of the TBL. The potential temperature of the mantle lies a thousand degrees below the right-hand side of the diagram!

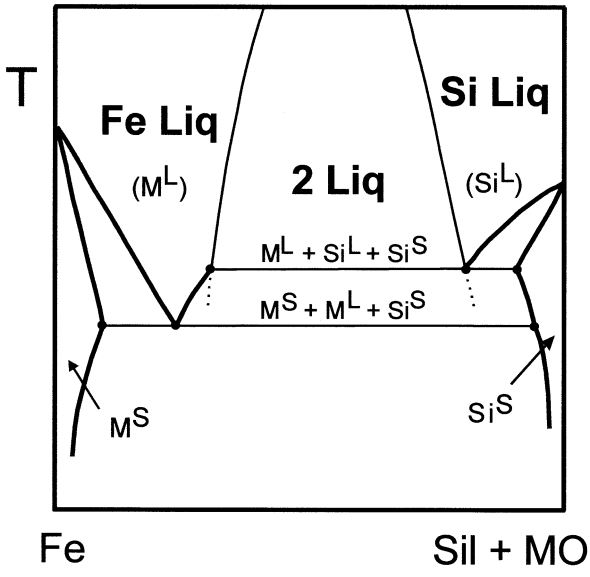

Fig. 1. Conceptual phase diagram for the CMB. The end members are Fe, representing the core metal, and Sil + MO, representing the silicate perovskite and MO (magnesiowüstite) of the mantle. The diagram is not intended to be true to scale but instead operationally adequate; the mutual solubilities are exaggerated. The phase relations are dominated by a large miscibility gap (2 Liq) separating silicate melt (Si Liq) from metal melt (Fe Liq) so as to reflect the limited mutual solubility of these two phases. M^S = metal crystals; M^L = metal melt; Si^S = mantle crystals; Si^L = mantle melt.

2.2. Conceptual Phase Diagram

In the temperature–composition phase equilibrium diagram of Figure 1, the end members are Fe as proxy for core metal on the left and silicate perovskite and MO on the right, representing the mantle. The mutual miscibilities of the solid phases are exaggerated for convenience of illustration. A large field of liquid immiscibility dominates the diagram and restricts the mutual solubilities of the end members. This field is reminiscent of the miscibility gap between liquid iron and liquid iron oxide at 1 atm in the system iron–wüstite (Darken and Gurry, 1946; see also Presnall, 1995). Such an immiscibility must occur unless it is to be supposed that silicate mantle and metal core melts are supercritical and infinitely miscible, a hypothesis hardly warranted by the seismic information.

Figure 1 illustrates several important principles embodied in the conjugate lines (tielines) that delineate three-phase equilibria. First, the metal melt that causes melting in the mantle is superheated (and superenriched in incompatible, low-melting components such as Mg, Si, and O) with respect to its own crystals (upper conjugate line). Second, the solid mantle is a crucible for the metal melt when that is saturated with its own crystals (lower conjugate line), as well as at higher temperatures in the two-phase field. Third, the upper left portion of the diagram illustrates the inner-core equilibrium between metal crystals and enriched melt that contains rejected solute (RS; all the components of the melt that do not enter the crystals). Fourth, the right-hand portion of the diagram illustrates the maximum solubility of metal in the mantle crystals in contact with metal melt, declining through the two-phase field and then along the solvus as cooling proceeds. The third and fourth points are emphasized in the cartoon of Figure 2.

In Figure 2, the mantle solvus represents the mantle as a refractory crucible for metal melt at temperatures below T_1, at which a giant silicate magma chamber might be generated in the base of the mantle. The conjugation line at T_2 is the core–mantle solidus. If any metal crystals exist here, they are caused by the mantle chilling the core, and they may induce a cool plume carrying material downward into the core. There is some seismic evidence for such T_2 crystal-melt equilibria. Thin rigid zones at the top of the core have been detected by Rost and Revenaugh (2001), who speculate on the coexistence there of solid Fe alloys and liquid metal. Any metal along the solvus below T_2 represents metal exsolved from the mantle as it cools.

The freezing of the inner core is symbolically represented by the tieline ICB in Figure 2. More realistically, the entire dia-

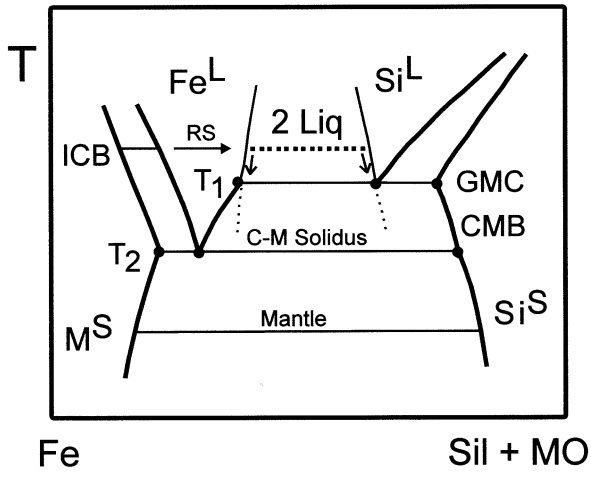

Fig. 2. Cartoon of Figure 1 showing, at left, the equilibrium at the ICB, and at right, the solvus for the mantle at the CMB. The ICB tieline represents the inner core at the solidus, and the silicate-oxide content of the outer core at the liquidus; sulfur and other diluents are not represented here. Arrows represent pathways of RS from the ICB to the mantle. Other abbreviations as in Figure 1.

gram lies at a much higher temperature at the ICB and slides down to the CMB temperature at the top of the core. Nevertheless, the result of inner core freezing can be illustrated in Figure 2 as metal melt being isothermally enriched in RS (i.e., perovskite and MO components) from the ICB tieline: see the arrow. In the extreme, this enriched material encounters the two-liquid solvus, and light mantle melt exsolves from it (dotted tieline in Fig. 2). As the mantle cools the core melt, further exsolution takes place (arrows in the two-liquid field) until the three-phase equilibrium is reached at T_1. Only here can the silicate melt deposit mantle crystals on cooling. Below this temperature, the mantle is a refractory crucible for the molten core until the lower three-phase equilibrium is reached at T_2. At still lower temperatures, solid mantle and solid metal are exsolved from one another (e.g., the tieline labeled "Mantle").

3. ANALOGIES FROM SILICATE MAGMAS

3.1. Comparisons between Silicate and Metal Magmas

The approach to this discussion stems from studies of solidification in silicate magma chambers, principally the Kiglapait intrusion (Morse, 1969, 1979a, b, 1986a, 1988). In these and other contributions, some success was achieved in identifying and quantifying adcumulus growth with and without compositional convection. But silicate melt is not metal melt, and rock is not iron. Nevertheless, among several physical properties relevant to crystal nucleation and growth, only the density, viscosity at the basal outer core, and perhaps the chemical diffusivity are significantly different for mafic melts in crustal magma chambers and in the core, respectively. Comparisons are shown in Table 1, where entries are based on well-known or commonly assumed values that can be found in the literature (e.g., Turcotte and Schubert, 1982); less common estimates are specifically cited in the table. The citation PREM refers to the Dziewonski and Anderson (1981) Preliminary Reference Earth Model, as reduced in Stacey (1992). Of particular interest are the viscosity and chemical diffusion coefficient, which relate to how easily solute may be removed during crystal growth. The viscosity and diffusion entries in Table 1 directly support the relevance of magma chamber principles to solidification near the top of the outer core.

The recent viscosity and diffusion estimates for the core are based on self-diffusion of ^{57}Fe in liquid iron up to 16 GPa and 2373 K (Dobson, 2001), and for the pressure at the ICB, they are very different from those in mafic magmas. These values are likely to be extreme for two reasons. First, the activation volume found by Dobson at lower pressures is treated as constant in the extrapolations to ICB pressures, but it is more likely to be compressible. Second, self-diffusion of Fe is not necessarily a limiting condition for light elements such as S, O, Mg, or Si, any of which might be expected to diffuse faster than the host Fe. It is these elements, rejected from the freezing surface of the inner core, that matter to the mode of solidification there.

3.2. Principles of Solidification

The study of the accumulation and solidification of silicate and oxide crystals from the melt has formed a robust part of igneous petrology since H. H. Hess (1939) deduced the process of adcumulus growth. This is the process named by Wager et al. (1960) to describe the isothermal, isocompositional solidification of an initially porous crystalline sediment (or cumulate) from the melt, by exchange with an infinite magma reservoir. Solidification may occur through diffusion in the melt alone or

Table 1. Comparison of properties.

Crustal mafic magma	Core melt
Viscosity, Pa s:	Same at CMB; higher at ICB:
1-20; (e.g., Kushiro, 1980) Lowest for high pressure and picrites	CMB: 10 (Dobson, 2001) ICB: 10^3 (Dobson, 2001)
Diffusion coefficient, m^{-2} s^{-1}	CMB same: 1.3×10^{-11} (^{57}Fe, Dobson, 2001)
10^{-11} for Mn, Fe, Ca in basalt (Brady, 1995)	ICB: In flux! 3×10^{-9} (Fearn et al., 1981) BUT: 4×10^{-15} (^{57} Fe, Dobson, 2001)
Thermal expansion coefficient, K^{-1}	Same:
10^{-5}	10^{-5} (Stacey, 1992)
Density, 10^3 kg m^{-3}	Very different!
<3	CMB: 10; ICB: 12.17 (PREM)
Density change on melting, percent	Same:
4–7 (Morse, 1979a)	ICB: 5 (PREM; 12.76 in IC)

aided by compositional convection (Braginsky, 1963). Solidification and accumulation therefore compete: if accumulation occurs too fast, the adcumulus growth process cannot keep up, and the trapped melt occurs as a residual porosity ($p_r > 0$). But if accumulation is slow enough, adcumulus growth may proceed to near perfection ($p_r \sim 0$), so that solidification occurs at the cumulate interface.

3.2.1. Adcumulus Growth

The limiting criterion for essentially perfect adcumulus growth occurs in silicate magmas for felsic (light) cumulates on a flat floor, where stagnation impedes solidification because the RS is denser than the parent melt and must be expelled by diffusion alone. This criterion has been determined from analysis of field data to be an accumulation rate of ~0.5 to 1.0 cm/yr (Morse, 1979b, 1986a).

Considerable evidence of adcumulus solidification accrues from silicate cumulates deposited slowly over a timescale of approximately a million years, as in the Kiglapait intrusion (Morse, 1986a). Mafic basal cumulates rich in olivine reject a light solute, and they can be shown locally to have solidified before more felsic cumulates in the same package, for which the RS is dense (Morse, 1969). In such cases, the brittleness of the mafic layers can be attributed to their isothermal solidification by compositional convection, whereas the felsic layers solidified later and polythermally, retaining a significant residual porosity p_r that is now represented by zoned plagioclase.

Parts of the "Main Ore Band" in the Upper Zone of the Kiglapait intrusion consist of cumulus Fe-Ti oxide grains in a rock devoid of silicate, and of the order of 10 cm thick (Morse, 1980). Clearly, the adcumulus growth process has worked to perfection in the silicate-absent layer. Here the RS is rich in feldspar and mafic silicates, and hence light and easily removed upward.

A particularly compelling test of the adcumulus growth systematics arises from the successful correlation of the more porous roof-chilled rocks of the Kiglapait Upper Border Zone (UBZ) with the floor cumulates (Morse and Allison, 1986). This correlation was done by correcting for residual porosity in the UBZ, as estimated from zoning in plagioclase. When this correction was made, the appearance of apatite in the UBZ was found to occur at a plagioclase composition not demonstrably different from that in the layered group. The results could then be extended to other minerals, and to a general correlation between maximum anorthite content (An) in the UBZ with average An in the layered floor cumulates. Such a successful test demonstrates the power of cumulate theory where it can be appropriately applied and validates the quantification of cumulate solidification.

3.2.2. Calibration of Cumulate Types

A further test of adcumulus growth rates is afforded by experimental studies of crystallization in mixtures of natural Kiglapait minerals approaching inferred parent liquid compositions. Unzoned plagioclase crystals up to 50 μm across were grown from the melt in runs from 24 to 40 h in duration (Fig. 3), at rates of approximately 1 cm/yr (Sporleder, 1998). Because of barriers to tetrahedral diffusion in plagioclase, crystals

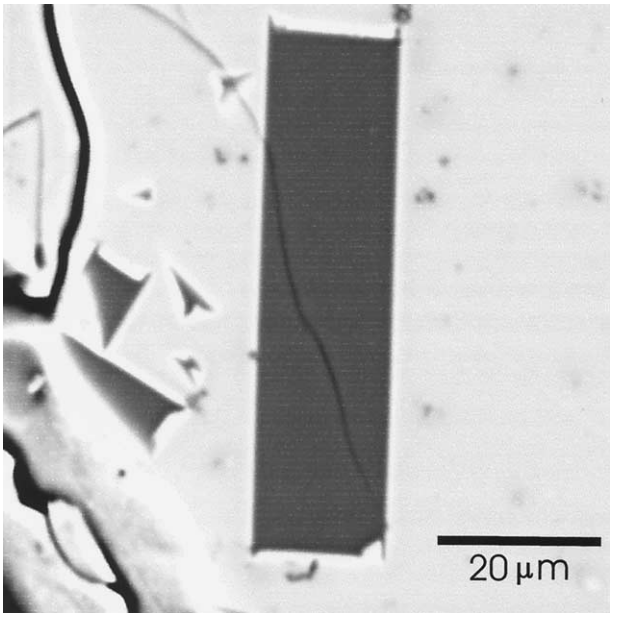

Fig. 3. Back-scattered electron image of an unzoned plagioclase feldspar grain experimentally grown at 1242°C at 5 kb for 24 h in molten troctolite approximating the bulk composition of the Kiglapait intrusion (Sporleder, 1998, run 6a.1).

of that phase cannot grow by dry reactive equilibrium crystallization in geologic, let alone laboratory time (Morse, 1984), and so must have grown by adcumulus growth, possibly aided by compositional convection. Plagioclase is the most refractory silicate in common rocks, and its resistance to homogenization is well known for its ability to record magmatic history.

The solidification of cumulates relative to accumulation rate is summarized in Figure 4, in which the several types of cumulates discussed by Wager et al. (1960) are evaluated in terms of their observed residual porosity (Morse, 1979b). Orthocumulates are those in which most or all of the initial porosity p_i is trapped to form ophitic textures and zoning on earlier cumulus grains. Adcumulates are those in which the residual porosity is minor or negligible, and represented only by trace amounts of excluded (i.e., not cumulus) minerals. Mesocumulates are rocks with intermediate texture. No fixed limits to these classes are needed, but in general, the central characteristics of 100 p_r ~30, 10, and 3% might be appropriate.

In the Lower Zone of the Kiglapait intrusion, the residual porosity was calibrated by the modal trace amounts of excluded (noncumulus) minerals and by zoning in plagioclase (Morse, 1979b), and it turned out that p_r varied systematically with stratigraphic height from 0.14 (14%) to 0.03 over the interval 0 to 84% solidified. This progression was then found to be correlated with accumulation rate, as calculated from the cooling history, thus establishing a working calibration for the success of solidification by adcumulus growth as a function of accumulation rate. This is the calibration shown in Fig. 4.

Although Figure 4 refers to solidification achieved solely by diffusion of relatively dense RS away from the solidification interface, it is unclear whether compositional convection played a part in the solidification of the Kiglapait cumulates, because the rocks exposed today accumulated on a sloping

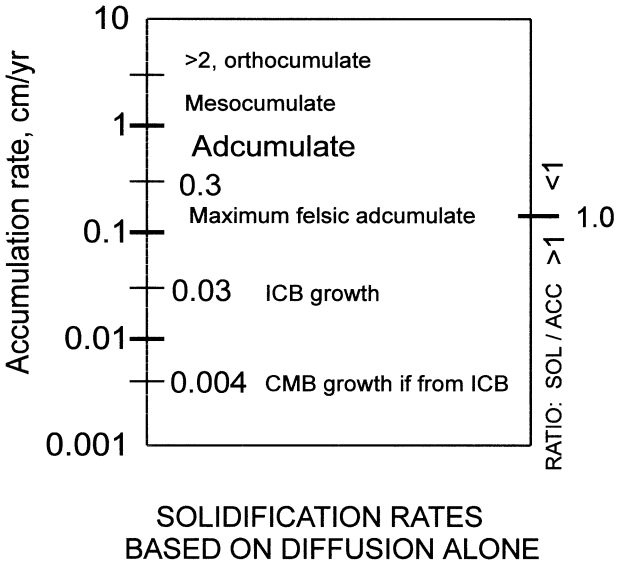

Fig. 4. Accumulation rates of different types of cumulates, compared with growth of boundary layers of the outer core. The ratio of solidification to accumulation rates is plotted at the right side of the diagram, assuming solidification by diffusion alone, without the help of compositional convection.

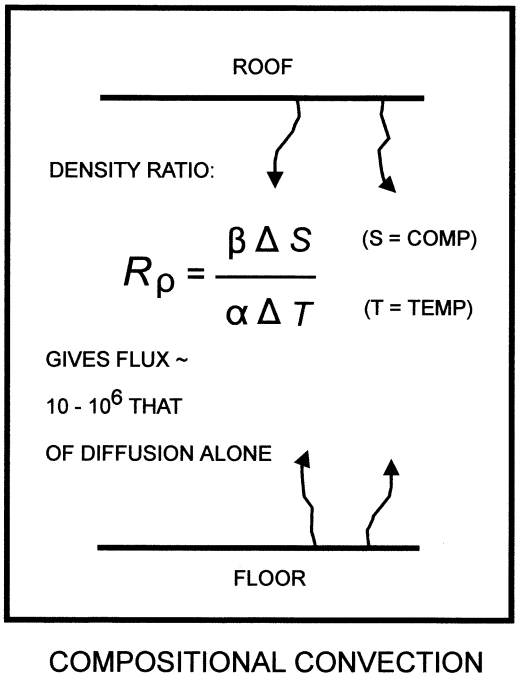

Fig. 5. Effect of compositional convection on solidification at a floor or roof. The density ratio of Turner (1965) is a measure of the tendency of compositional convection to overwhelm thermal convection.

floor along which RS would have tended to drain. However, the roof rocks formed in the TBL of the UBZ retain a high residual porosity despite their roof position and the rejection of moderately dense solute (Morse and Allison, 1986), so it is inferred that the floor cumulates benefitted relatively little from downslope removal of RS during their solidification.

In general, however, it is certain that when the RS is light, its escape from the floor dramatically enhances solidification and heat transport, as in the dunite layers referred to above. This effect is also shown in the Rum intrusion where melt corrosion at the roofs of sills has been aided by the short-circuit of latent and sensible heat transported by compositional convection from the solidifying olivine cumulate at the floor (Morse, 1986c; Morse et al., 1987).

3.2.3. Effects of Compositional Convection

Analysis of the Kiglapait data allowed the evaluation of the effects of compositional convection as well as adcumulus growth by diffusion. The treatment of adcumulus growth by Morse (1986a) is based on the concept of the competition between compressions and expansions due to compositional change and thermal effects, expressed as the density ratio of Turner (1965): $R_\rho = \beta\Delta S/\alpha\Delta T$, where $\beta\Delta S$ is the effect of composition on liquid density, composed of an expansion coefficient β and a compositional change ΔS. The term $\alpha\Delta T$ is the analogous effect of temperature on liquid density and α is taken as 10^{-5} deg^{-1}. The compositional term may be combined as a compression (or expansion) and the density ratio itself can also be considered without regard to sign as a measure of the escaping tendency of RS from a solidifying interface. Whereas the density ratio was evaluated at 1 to 5 for basaltic magmas in general (Huppert and Sparks, 1980), on the basis of the Kiglapait analysis, it can reach values from 6 to 10^6 (Morse, 1986a), showing dramatic escaping tendencies compatible with roof melting in certain circumstances. Figure 5 is a cartoon summarizing the opposite effects of compositional convection near a mafic floor and near a felsic roof.

4. NO MUSHY ZONE AT THE ICB

Opinions on the nature of the ICB differ radically, ranging from dendritic and highly porous to hard ground with a microscopically thin transition from melt to solid. Such calculations come from two diverse approaches, one theoretical and one empirical. The end-member results can be taken for the present purpose as embodied in the theoretical approach of Fearn et al. (1981) and the empirical approach of Morse (1986b). In the former work and its descendants (e.g., Bergman, 1997), it is concluded that constitutional supercooling occurs at the ICB and causes dendritic growth. In the latter work, it is concluded instead that adcumulus growth operates at zero supercooling to form a solid interface. Both approaches assume compositional convection to transport the RS upward, as proposed by Braginsky (1963) to drive the dynamo. The results reached by the two schools differ by a factor of somewhere between 10^5 and 10^8. We appear to have a problem here.

Fearn et al. (1981) calculated a critical inner core growth rate for supercooling and compared that to the actual growth rate as determined for an inner core lifetime of 3 Ga. If the actual growth rate exceeds the critical rate, then constitutional supercooling occurs. They found that it does occur, chiefly because they found a very low threshold for the critical growth rate.

4.1. Inner Core Growth Rate

All estimates of inner core growth rate considered here lie within the same order of magnitude, and most of them simply depend on the lifetime chosen. Morse (1986b) used an average radial growth rate based on an inner core lifetime of 1.5 Ga (Stevenson, 1981; see also 1.6 Ga, Buffett et al., 1992), yielding a mean radial growth of ~0.07 cm/yr. For a longer lifetime of 2.7 Ga (Hale, 1987; Selkin et al., 2000), the result is 0.05 cm/yr. Buffett et al. (2000) used a nicer approach based on root time, with a lifetime of 2 Ga, yielding a radial growth rate of 0.03 cm/yr today (0.0226 cm/yr for a lifetime of 2.7 Ga, or 0.0204 cm/yr for a lifetime of 3.0 Ga). Fearn et al. (1981) used a constant time-averaged mass increment of 5×10^{-8} kg m^{-2} s^{-1}, which translates to a constant radial increment of 0.0124 cm/yr, assuming a mean density of 1.269×10^{4} kg m^{-3} (PREM; Stacey, 1992). Such a growth rate exceeds the critical condition as calculated by Fearn et al. (1981)—that is, 10^{-10} kg m^{-2} s^{-1}, as discussed below.

4.2. Results from Diffusion and Stokes Flow

The criterion for adcumulus growth requires an accumulation rate lower than the solidification rate, as discussed above. This criterion must therefore be a lower bound for the critical growth rate for constitutional supercooling because adcumulus growth removes porosity quantitatively. This is the principle that informed the evaluation of escape velocities from the ICB by Morse (1986b), who noted that his results were comparable to those of Stevenson (1986) for Mercury after adjustment for g. Morse (1986b) calculated the removal of RS from the ICB by diffusion and then by Stokes flow, assuming a boundary layer 1 cm thick—that is, some 33 times the annual growth increment. He used values for the diffusion coefficient and viscosity that are out of date, but for the sake of comparison, the 1986 result yielded an ascent velocity of order 1 cm/s (864 m/d). Recalculation with the newest parameters in Table 1 yields, for the characteristic diffusion distance $x = (\mathrm{Dt})^{0.5}$ and t = 1 d, $x = 1.93 \times 10^{-3}$ cm. The Stokes law calculation for $r = 1$ cm, $\Delta\rho = -0.04$ g cm^{-3}, $g = 420$ cm s^{-2}, $\nu = 813$ stokes (for $\eta = 10^{3}$ Pa s $= 10^{4}$ poise and $\rho = 12.3$ g cm^{-3}) gives $V = -4.592 \times 10^{-3}$ cm s^{-1}, and if run for 1 d at this terminal velocity, a distance traveled of 397 cm. As is characteristic of compositional convection, this transport result is $\sim 2 \times 10^{5}$ times more effective in removing RS than chemical diffusion alone.

4.3. Results from the Density Ratio

The density ratio of Turner (1965), $R_\rho = \beta\Delta S/\alpha\Delta T$, describes the relative efficiency of compositional to thermal effects on density. The density ratio can be used crudely as a multiplier on the thermal diffusivity to estimate the relative importance of compositional convection, as with Stokes flow compared with chemical diffusion cited above.

The density ratio can be evaluated for the ICB by using published approximations. The specific volume change with composition (Fearn et al., 1981), equal to 9.2×10^{-5}, can be taken as the numerator $\beta\Delta S$. A maximum value of $\alpha\Delta T$ results if ΔT is taken as the outer-core adiabat at the ICB, 1.0 K km^{-1} or 10^{-7} K cm^{-1} (Stacey, 1992). Then $\alpha\Delta T = 10^{-12}$ K cm^{-1}, and $R_\rho \geq 9.2 \times 10^{7}$. The true gradient must be somewhat greater, at least to the slope of the two-phase saturation curve, so R_ρ must be $>10^{8}$. The result vastly exceeds the criterion for thriving adcumulus growth.

4.4. The Case for Constitutional Supercooling

In the Fearn et al. (1981) calculation of the critical radial growth velocity for constitutional supercooling, the numerator in their eqn. 5 combines the diffusion coefficient and some other unexceptionable considerations with compositional expansion, with the result that its 1981 value is within an order of magnitude of the expansion itself, expressed as the specific volume change with composition. The value for the entire numerator is 1.1×10^{-5}, similar to $\beta\Delta S$, above. Therefore, we were in substantial agreement about the numerator. However, the critical term in their numerator is the diffusion coefficient, which has changed downward by six orders of magnitude since their analysis (Table 1 and see below).

Fearn et al. (1981) stated that in their eqn. 5 they neglected a thermal term as negligible. However, a small but perhaps not negligible thermal term in the denominator of the density ratio has a very large influence on that ratio (as above). By contrast, Fearn et al. (1981) introduced into their denominator an energy of mixing taken as 4.4×10^{7} J kg^{-1}. This results in a denominator of order 10^{5}, driving the whole equation to a very small number as the criterion for constitutional supercooling. Their critical growth rate of 10^{-10} kg m^{-2} s^{-1} is smaller by a factor of 500 than their estimated actual growth rate. This result predicts constitutional supercooling. With the new diffusion coefficient (Table 1), the result is reduced by six orders of magnitude and is hence even more strongly in favor of constitutional supercooling. But as noted in section 4.1, this low value for the diffusion coefficient must be considered a minimum estimate, and the associated derived viscosity, a maximum.

So what's wrong here? Clearly the mixing energy of order 10^{7} overwhelms the Fearn et al. (1981) result, and we may inquire whether that is appropriate or reasonable. This question, in turn, brings to the fore the matter of what happens to the RS from the ICB. The authors (p. 232) reasoned that "fluid motions are inhibited at the rigid freezing boundary" and therefore that the "fluxes…of light material…and heat…must be removed from the interface by diffusion." Here they combined material diffusion with a "barodiffusive flux" (i.e., compositional convection) in their eqns. 3 to 5. By treating compositional convection as a diffusive flux, they limited their considerations to the immediate vicinity of the freezing boundary. That may be why they introduced the energy of mixing.

However, convection is not diffusion but instead a material transport, as emphasized by the treatment of Turner (1965). If compositional convection occurs with such power as to drive the dynamo, then surely it escapes the ICB with appreciable velocity, over a characteristic distance of perhaps 100 m (Dobson, 2001). If so, then it does its mixing by dissipation far away from the ICB, and the energy of mixing must therefore be of no consequence in the immediate vicinity of the ICB. One may therefore conclude that as a criterion for supercooling at the ICB, a large value for the energy of mixing is inappropriate; a

value near 1.0 might be far more realistic. It's the boundary layer that counts! Accordingly, with the new diffusion coefficient but without the energy of mixing, the calculated critical growth rate is reduced to 50 times the estimated actual growth rate, and constitutional supercooling still wins, but it is highly vulnerable to future adjustments to the diffusion coefficient.

4.5. Recapitulation

Both the updated 1986 results, from Stokes Law and from the density ratio, strongly predict adcumulus growth with compositional convection. In fact, diffusion alone yields removal of RS a distance of 0.037 cm/yr, similar to the growth rate of 0.03 cm/yr. If compositional convection works at all, it must favor adcumulus growth. The result in section 4.4 is the only one that disagrees with this conclusion, and it is at risk of revision, both from uncertainties in the diffusion coefficient and from neglect of a thermal term.

Viscosity is a critical feature for comparison of silicate magma and for the liquid core at the ICB. The high end of the range for silicate magmas (20 Pa s; Table 1) applies to olivine tholeiite at low pressure, a good proxy for the Kiglapait magma, but it is 50 times lower than that listed in Table 1 for the ICB. However, the viscosity at the ICB pressure is calculated from the diffusivity and is vulnerable to the same uncertainties mentioned above regarding extrapolation from lower pressures. The data of Dobson (2001) are the most relevant available today, but historical estimates of outer core viscosity have varied over 14 orders of magnitude (Secco, 1995), so even great data need to be used with caution.

Nucleation and growth of metal crystals from metal melt are well-known phenomena lying at the other end of the spectrum from plagioclase, requiring in extreme cases a centrifuge method to achieve a quench. If plagioclase feldspar can grow isocompositionally and isothermally in the Earth's crust and in the laboratory at growth rates of ~1 cm/yr, then metal crystals at the liquidus surely ought to do so with the help of compositional convection at a growth rate of 0.03 cm/yr at the ICB. The growth criterion of Fearn et al. (1981) is unlikely to be appropriate to the growth of the inner core.

4.6. Freezing at the ICB

The ICB advances by the extraction of heat from the core. This is aided by the upward transport of latent heat away from the ICB by compositional convection, with its ultimate extraction from the core into the mantle. It is also aided by the return flow of cooler metal melt needed to induce crystallization. In principle, the core can freeze at the CMB (T_2, Fig. 2) and send cool plumes downward, but it would be unlikely for a two-phase, solid-liquid slurry to survive transit of the whole outer core. However, the memory of a cooler temperature must eventually survive a downward transit. A convenient way of representing this action is by shifting the outer core adiabat down-temperature by a small amount δT (Fig. 6). Now the adiabat intersects the melting curve above the ICB to form a nucleation zone (NZ) in which crystals might nucleate and grow.

Crystal nucleation classically involves some amount of undercooling, in contrast to growth, which originates at zero undercooling. However, the nucleation of metal crystals from the melt generally requires a microscopically small undercooling. In a sheared liquid, mechanical eddies and dislocations can furnish sites for heteronucleation. The nucleation of metal crystals is, therefore, expected to occur where the adiabat touches the liquidus. If it does not occur there, it will do so at some small undercooling represented by transit across the liquidus.

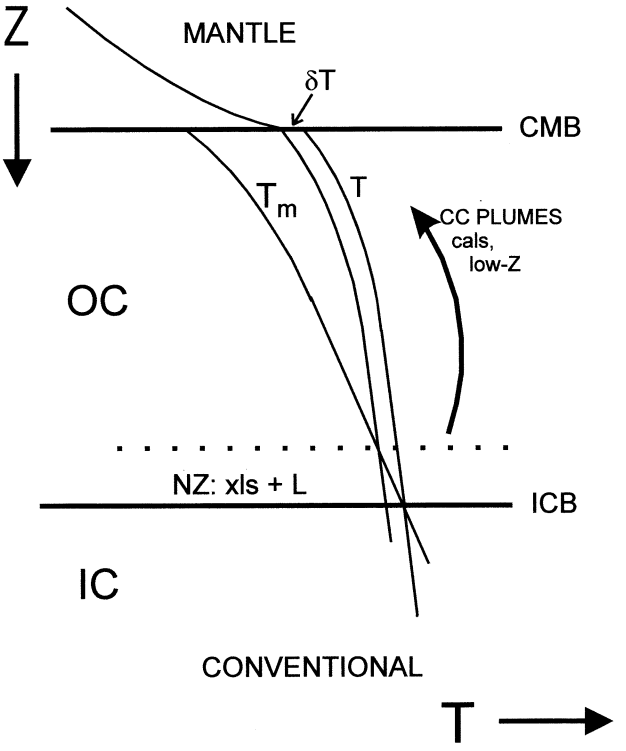

Fig. 6. Conventional cooling of the outer core at the CMB to allow freezing at the ICB. The T-Z curves are distorted from Stacey (1992, p. 336). The curve T represents the core adiabat. The slight cooling δ T is considered to propagate to the region of the ICB, creating a NZ, where it crosses the melting curve T_m. CC = compositional convection; cals = calories; IC = inner core; low-Z = light elements; xls = crystals; L = liquid; OC = outer core. This scenario is conventional in the sense that it ignores cooling of the core to the liquidus at the CMB, which might, however, occur at certain times and places (Rost and Revenaugh, 2001).

An enlargement of the ICB region is shown in Figure 7. A short metastable transit of the adiabat across the liquidus (T_m) into the NZ is shown. Nuclei are assumed to form somewhere in the NZ. The growth of crystals then releases latent heat, returning the temperature to the liquidus. By analogy with the weather, this condition is often called a "wet adiabat," whereas more accurately it is simply a two-phase saturation curve. If nucleation and crystal growth rates are very small, the actual configuration may be a "damp adiabat" slightly off the saturation curve; but at the ICB, two-phase saturation is guaranteed. The ICB interface thereafter moves outward as long as heat is removed.

The process of crystal growth at the ICB is so slow that it may involve contemporaneous annealing and growth of very large crystals aided by adcumulus growth. Sizes of hundreds of meters have been suggested (Bergman, 1998). However, the

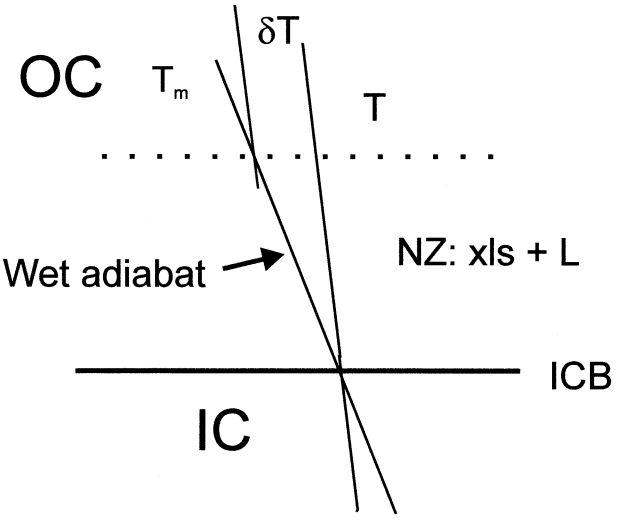

Fig. 7. Detail of the NZ near the ICB. Symbols as in Fig. 6.

opportunities for nucleation may well lead initially to the settling of small grains.

5. FURTHER DISCUSSION OF THE INNER CORE

5.1. Inner Core Isotropy

One motivation for the idea that the inner core might be dendritic stems from the interpretation of seismic observations that the inner core is anisotropic, at least at some depth. If so, dendritic growth might explain the anisotropy. However, anisotropy has also been ascribed to an interaction with the magnetic field itself (e.g., Karato, 1993). In particular, Buffett and Wenk (2001) showed that an appropriate electromagnetic shear stress can lead to the required alignment of individual grains with their c-axes parallel to the equatorial plane. In addition, seismic evidence suggests that the outer 100 to 400 km of the inner core is isotropic (e.g., Creager and Ouzounis, 2000), and thus dendritic growth at the ICB can play no role in the acquisition of anisotropy.

5.2. Light Elements in the Inner Core

The composition of the inner core is uncertain; it may retain some light elements. Recent experimental observations (Li and Agee, 2001) favor sulfur over oxygen or silicon as the chief light element in the outer core, but as the authors noted, a full complement of ~10% S falls afoul of cosmochemical evidence as currently understood. Sulfur in the form of troilite nodules that were once trapped liquid occurs conspicuously in some iron meteorites such as Agpalilik, on display in the National Museum in Copenhagen (see Wasson, 1974). From such evidence, and the slim knowledge of a small density difference between the inner and outer parts of the core, it appears possible that some light elements reside in the inner core (which nevertheless is not an asteroid-sized object!). Such an eventuality may not by itself be found inconsistent with adcumulus growth at the ICB. Solidification at the interface may be the normal steady-state condition for the space- and time-averaged ICB, but there is no reason to suppose that the core is totally immune to such familiar chaotic events as cascades and avalanches. Such an irregular event might well bury the interface deep enough in crystals to inhibit adcumulus growth and generate a residual porosity. If this is in the form of troilite, however, it will be liquid for a time far into the future because the inner core is presently at a temperature far above the cotectic with sulfide crystals. Such a segregated melt would presumably wet the deforming core metal thoroughly (Rushmer et al., 2000) and tend to find its way out to the liquid core. Therefore, if a light element is to be considered for the inner core, it must either be refractory or kept down there by some unknown process. Carbon may fill the bill (Hillgren et al., 2000).

The fate of the light elements rejected at the ICB has been the subject of much conjecture, but the simplest answer is that the RS flux joins a mantle melt layer at the base of D″ and flows wherever that goes (Morse, 2000). The temperature–composition pathway is illustrated by the arrows in Figure 2.

6. THE NUTATION PROBLEM AND THE CMB

6.1. Introduction

The coupling of the Earth's magnetic field to the rotation of the planet involves fluid motions in the outer core and the motion of conductive materials outside its fluid boundaries. These magnetic couplings in turn affect the Earth's nutations. When the Earth's axis nods along its precession path, the amplitude of the nutation is out of phase with tidal forcings. This problem was addressed in detail by Buffett (1992), who showed that the anomalous dissipation of the amplitude of nutation cannot be due to ocean tides or mechanical properties of the mantle. Instead, he showed that the discrepancy can be eliminated if the lowermost 200 km of the mantle has an enhanced electrical conductivity, which was attributed to the presence of iron from the core.

The hypothesis of a conducting layer at the base of the mantle was examined by Poirier et al. (1998), who found that it fared poorly. These authors considered both partial melting of the mantle, which contributed little to the conductivity, and infiltration of iron into the mantle, which would only affect a few meters. However, a larger-scale uptake of dissolved and reprecipitated metal by melted mantle was contemplated by Morse (2000) and solution rather than infiltration of iron is contemplated in the phase diagram of Figure 1.

In a later contribution, Buffett et al. (2000), suggested an origin for this metal-rich region of enhanced conductivity in a capture zone at the top of the core, where core metal is caught within porous flotation sediments at the top of the core, and then accreted to the mantle. Problems with this idea were raised by Morse (2001a,b) on the grounds of igneous solidification theory, and these problems are revisited below. However, rather than begin by plowing old ground, it will be fruitful to explore another way to enhance the electrical conductivity of the basal mantle. The problem still is how to capture conducting material in an insulating matrix in such a way as to yield a gradient from strong conductivity at the base of the mantle to a weaker value at some shallower depth.

6.2. Solubility

It is proposed here that metal is added to the basal mantle by first dissolving it at the core and then exsolving it within the mantle. The proposal rests on two recent observations: evidence for precipitation of metal from deep mantle minerals, and evidence that the MO phase is weak and coats perovskite in thin films at the base of the mantle. In addition, account is taken of the tectonite status of the mantle, and its recurrent visit to the core by convection.

Silicate melt and perovskite may both contain excess oxygen relative to the join MO-SiO_2. MO (or, specifically, magnesiowüstite) may dissolve Fe^o chiefly by oxidation to FeO, increasing the ratio of Fe to total metal in the MO phase at the expense of oxygen in a coexisting phase. Whether MO can also dissolve any appreciable amount of Fe^o at core pressures is not known. However, it can be assumed that silicate melt at the CMB is relatively metal rich and oxygen poor, becoming more oxidized at higher levels in contact with solid mantle (Morse, 2000; Fig. 2). To some degree, at least, the coexisting MO itself must share this transition.

Redox precipitation of metal from magnesiowüstite–perovskite assemblages and from olivine by reduction has been shown experimentally (Hirsch et al., 1993; Poirier et al., 1996; Duba et al., 1997), and might be expected to occur in mantle minerals near the core. Magnesiowüstite is considered to be the chief conductive phase in the lower mantle (Wood and Nell, 1991; Duba and Wanamaker, 1994). The most reduced and surely the hottest part of the mantle occurs in contact with the molten core, at the CMB, T_1 to T_2 in Figure 1. The redox condition there lies perhaps one or two log units below the iron–wüstite buffer (Li and Agee, 2001). The mantle phases are saturated with iron at the CMB. When carried away from the CMB in the deforming tectonite matrix of the lowermost mantle, the mantle phases will encounter lower temperatures. This transit will inevitably cause the precipitation or exsolution of metal.

The strength and viscosity of MgO end-member periclase are lower than those of $MgSiO_3$ perovskite, and these qualities make it likely to coat the perovskite matrix in continuous films. This was shown by Yamazaki and Karato (2001), who also showed that the large rheological contrasts between the phases persist in the ambient MO and $(Mg,Fe)SiO_3$ (perovskite) phases of the lower mantle. The weaker MO coats the perovskite, which in turn defines most of the bulk viscosity of the lower mantle.

If magnesiowüstite is the carrier of excess metal and it forms continuous films on perovskite in the basal layer of the mantle, then any metal precipitated from the MO phase should tend to be extended into ribbons, rather than dispersed grains. Such a configuration might supply a connectivity that would approach that of a continuous metal film. If so, it must significantly enhance the electrical conductivity of the basal layer. A residual metal content of ~5% in the lower 200 km of the mantle was considered by Buffett et al. (2000) to be adequate to explain the nutation effect, but the metal was considered dispersed from its origin in pore spaces. In a deforming, connected network, a lower metal content might suffice. Exsolution of metal from the core-saturated phases may be sufficient in amount and connectivity to account for the required electrical conductivity. If not, the deficit can perhaps be made up by physical entrainment of core metal in the deforming mantle, rather than by infiltration as considered by Poirier et al. (1998). Alternatively, metal deposition might occur from magma in the deep mushy zone near the roof of a giant CMB magma chamber, as previously suggested (Morse, 2000). Because the solubility of metal in melt exceeds that in mantle crystals (Figs. 1 and 2), a silicate melt is the most efficient agent for the transfer of Fe to the mantle. The high temperature of the core assures that the basal mantle must be transient at the CMB, and convect away from it continually. Therefore the lowermost mantle is expected to circulate into and out of contact with the core, refreshing its metal content on a secular basis.

In summary, enhanced electrical conductivity at the base of the mantle may be achieved by metal exsolved from mantle phases as they move away from core saturation with molten metal. The required connectivity can evidently be provided by continuous films of the oxide phase among deforming grains of the less-conductive silicate, as found for core metal in a deforming silicate matrix by Rushmer et al. (2000).

6.3. No Porous Sediments at the Roof of the Core

The report by Buffett et al. (2000) was a thought-provoking addition to a growing list of notions (Morse, 2001a,b) that the Earth's core may be losing material as well as heat to the overlying mantle. In it, the authors proposed that light elements rejected from the freezing inner core were accreted as flotation sediments at the top of the core. The sediments were given compositions of perovskite and MO, the same as the mineralogy of the basal mantle. The authors argued that such sediments could retain a porosity within which core metal could be captured and eventually accreted to the mantle. Such a porous, compacting mushy zone would be several kilometers thick and be built over some 10^5 years.

The expulsion of nonmetallic impurities from molten iron is an age-old study. But at the cooling rate of the core, any such slag material would be well crystallized. One may therefore assume growth of crystals from the melt, presumably immiscible silicate liquid, as in Figures 1 and 2.

Assuming with Buffett et al. (2000) that the volumes of RS and crystallized metal at the ICB are about equal, then the accumulation rate of sediment at the top of the outer core would be ~1/8 that of the growth rate of the inner core, hence ~0.004 cm/yr. For a mushy zone to be several kilometers thick, accumulation would have to have outpaced solidification for at least hundreds of millions of years. But the calibration of cumulate solidification (Fig. 4) suggests the opposite. Here also, where the viscosity is low and the chemical diffusivity relatively high (Table 1), solidification would be powerfully aided by compositional convection of dense, metallic RS, which would drain away from the sediment interface into the body of the outer core (Fig. 5). When the criterion for adcumulus growth is satisfied by orders of magnitude for diffusion alone, it is satisfied many times over in the presence of favorable compositional convection. There is therefore no basis for assuming a thick mushy zone with solidification by compaction at the CMB. Compaction cannot occur in a microscopically thin layer (Morse, 1986a).

6.4. No Freezing Where Melting

Both Williams and Garnero (1996) and Morse (2000) have discussed giant magma chambers at the CMB caused by melting the silicate mantle with heat from the core. Now we are considering deposition of the same silicate + MO mineralogy from the molten core at the same place and time. That the place must be the same is guaranteed by the fact that the short-circuit of heat transfer is run by the same compositional convection engine that contains the light elements that would crystallize to form the sediment. The core is either melting the mantle or freezing out onto it; we cannot have it both ways.

6.5. No Silicate Crystals below the CMB

Finally, direct deposition of silicates from the core is a thermal impossibility. The upper region of the liquid core is greatly superheated (Fig. 6) with respect to its own liquidus, which is certainly the liquidus of iron-rich metal (Fig. 1). It is therefore very far from any cotectic equilibrium with silicate material (see T_1 in Fig. 2). The only place where the liquid core metal coexists with silicate is in contact with the mantle (T_1 to T_2 in Fig. 2).

7. SUMMARY AND CONCLUSIONS

Solubility of iron in the mantle is greatest at the CMB and possibly can account for the precipitation of enough metal on cooling to yield a high electrical conductivity in the basal mantle. Conductivity is likely to be enhanced by connectivity due to smearing of the exsolved metal within the weak metal-oxide phase that coats perovskite grains in a deforming matrix. These conclusions are supported by a conceptual phase diagram for the CMB.

The light-element-enriched solute rejected from the freezing of the inner core is most likely added to the mantle by solution in molten silicate at the D″ layer. However, if it crystallizes at the CMB, it must do so from an immiscible silicate melt expelled from the iron melt of the outer core. Little opportunity exists for any accumulation of new silicate-MO crystals at the base of the mantle, but no opportunity exists for any porous cumulate to develop because the cumulate must solidify as it is deposited, by adcumulus growth strongly aided by compositional convection. The physical properties of mafic silicate melts in the crust, and metal melt at the top of the core, appear to be so similar that the solidification of observable mafic cumulates furnishes a reliable guide to CMB processes.

The freezing of the inner core is also aided by compositional convection, and the growth rate there is many times slower than needed to cause adcumulus growth. Here the physical properties of the melt are less obviously comparable to the parents of observable cumulates, and the relevant parameters are still in a state of development. Estimates of critical growth conditions are therefore less robust. The bottom line is that even at the lowest estimate of diffusivity, the removal of RS by diffusion alone is comparable to the growth rate of the inner core, so that any compositional convection at all must guarantee adcumulus growth. If compositional convection can drive the dynamo, it can drive adcumulus growth of the inner core.

It is interesting to note that writers on the core treat compositional convection mainly or exclusively in terms of its energy of mixing, which provides heat to drive the dynamo. However, the first action of compositional convection at a solidification front is the material transport of evolved solute carrying latent heat away from the growing interface. This action, unlike diffusion, amounts to a short circuit for heat, hence the emphasis on heat pumping (Morse, 1986c, 2000). One may grant that over the megameters of transit distance in the outer core, the solute may become well mixed, liberating heat. Near the surface it will unmix again (Fig. 2) with the absorption of heat. But will the solute always and everywhere mix completely? On a planet with a Gulf Stream, a North Atlantic Deep Water, and an Equatorial Countercurrent that has the aspect ratio of a cigarette paper seen end-on, I wouldn't bet on it.

Acknowledgments—Hat Yoder was a generously supportive influence during my graduate school days and through a fruitful fellowship that he sponsored at the Geophysical Laboratory. He spent the evening of his 40th birthday at our shabby digs in Montreal, leaving Dorothy and me chagrined that we had not held a celebration. Now that he has reached 80, we are at last catching up, and I hope this contribution will stimulate the juices once again. I thank Mike Bergman, John Brady, Al Duba, David Dobson, Gary Lofgren, Anne Hofmeister, Jie Li, and an anonymous reviewer for helpful discussions and comments. The research was supported in part by NSF grant EAR-9526262.

Associate editor: C. R. Neal

REFERENCES

Bergman M. I. (1997) Measurements of elastic anisotropy due to solidification texturing and the implications for the Earth's inner core. *Nature* **389,** 60–63.

Bergman M. I. (1998) Estimates of the Earth's inner core grain size. *Geophys. Res. Lett.* **25,** 1593–1596.

Brady J. B. (1995) Diffusion data for silicate minerals, glasses, and liquids. In *Mineral Physics and Crystallography* (ed. T. J. Ahrens), pp. 269–290 AGU Reference Shelf 2..

Braginsky S. I. (1963) Structure of the F layer and reasons for convection in the Earth's core. *Doklady Akademiya Nauk SSSR* **149,** 8–10.

Buffett B. A. (1992) Constraints on magnetic energy and mantle conductivity from the forced nutations of the Earth. *J. Geophys. Res.* **97,** 19581–19597.

Buffett B. A., Huppert H. E., Lister J. R., and Woods A. W. (1992) Analytical model for the solidification of the Earth's core. *Nature* **356,** 329–331.

Buffett B. A., Garnero E. J., and Jeanloz R. (2000) Sediments at the top of the Earth's core. *Science* **290,** 1338–1342.

Buffett B. A. and Wenk H.-R. (2001) Texturing of the Earth's inner core by Maxwell stresses. *Nature* **413,** 60–63.

Buffett B. A., Garnero E. J., and Jeanloz R. (2001) Response. *Science* **291,** 2092.

Creager K. C. and Ouzounis A. (2000) Homogeneous isotropy and heterogeneous anisotropy of the inner core. *EOS Trans. AGU* **81,** F884.

Darken L. S. and Gurry R. W. (1946) The system iron–oxygen. II. Equilibrium and thermodynamics of liquid oxide and other phases. *J. Am. Chem. Soc.* **68,** 798–816.

Dobson D. P. (2001) Pressure dependence of self-diffusion in liquid Fe: Implications for outer core convection. *J. Conference Abstr.* **6,** 426.

Duba A. G. and Wanamaker B. J. (1994) DAC measurement of perovskite conductivity and implications for the distribution of mineral phases in the lower mantle. *Geophys. Res. Lett.* **21,** 1643–1646.

Duba A. G., Peyronneau J., Visocekas F., and Poirier J.-P. (1997) Electrical conductivity of magnesiowüstite/perovskite produced by laser heating of synthetic olivine in the diamond anvil cell. *J. Geophys Res.* **102,** 27723–27728.

Dziewonski A. M. and Anderson D. L. (1981) Preliminary reference Earth model. *Phys. Earth Planet. Inter.* **25,** 297–356.

Fearn D. R., Loper D. E., and Roberts P. H. (1981) Structure of the Earth's inner core. *Nature* **292,** 232–233.

Garnero E. J. and Helmberger D. V. (1996) Seismic detection of a thin laterally varying boundary layer at the base of the mantle beneath the central Pacific. *Geophys. Res. Lett.* **23,** 977–980.

Hale C. J. (1987) Palaeomagnetic data suggest link between the Archaean–Proterozoic boundary and inner core nucleation. *Nature* **329,** 233–237.

Hess H. H. (1939) Extreme fractional crystallization of basaltic magma: the Stillwater igneous complex. *Trans. Amer. Geophys. Union,* 430–432.

Hillgren V. J., Gessmann C. K., and Li J. (2000) An experimental perspective on the light element in the Earth's core. In *Origin of the Earth and Moon* (eds. R. M. Canup and K. Righter), pp. 245–263. University of Arizona Press.

Hirsch L. M., Shankland T. J., and Duba A. G. (1993) Electrical conduction and polaron mobility in Fe-bearing olivine. *Geophys. J. Int.* **114,** 36–44.

Hofmeister A. M. (1999) Mantle values of thermal conductivity and the geotherm from phonon lifetimes. *Science* **283,** 1699–1706.

Huppert H. E. and Sparks R. S. J. (1980) The fluid dynamics of a basaltic magma chamber replenished by an influx of hot, dense ultrabasic magma. *Contrib. Miner. Petrol.* **75,** 279–289.

Karato S.-I. (1993) Inner core anisotropy due to the magnetic field-induced preferred orientation of iron. *Science* **262,** 1708–1711.

Kushiro I. (1980) Viscosity, density, and structure of silicate melts at high pressures, and their petrological applications. In *Physics of Magmatic Processes* (ed. R. B. Hargraves), pp. 93–120. Princeton University Press.

Li J. and Agee C. B. (2001) Element partitioning constraints on the light element composition of the Earth's core. *Geophys. Res. Lett.* **28,** 81–84.

Marsh B. D. (1996) Solidification fronts and magmatic evolution. *Mineral. Mag.* **60,** 5–40.

Morse S. A. (1969) *The Kiglapait Layered Intrusion, Labrador*. Geological Society of America Memoir 112.

Morse S. A. (1979a) Kiglapait geochemistry I: Systematics, sampling, and density. *J. Petrol.* **20,** 555–590.

Morse S. A. (1979b) Kiglapait geochemistry II: Petrography. *J. Petrol.* **20,** 591–624.

Morse S. A. (1980) Kiglapait mineralogy II: Fe-Ti oxide minerals and the activities of oxygen and silica. *J. Petrol.* **21,** 685–719.

Morse S. A. (1984) Cation diffusion in plagioclase feldspar. *Science* **225,** 504–505.

Morse S. A. (1986a) Convection in aid of adcumulus growth. *J. Petrol.* **27,** 1183–1215.

Morse S. A. (1986b) Adcumulus growth of the inner core. *Geophys. Res. Lett.* **13,** 1557–1560.

Morse S. A. (1986c) A magmatic heat pump. *Nature* **324,** 658–660.

Morse S. A. (1988) Motion of crystals, solute, and heat in layered intrusions. *Can. Mineral.* **26,** 209–244.

Morse S. A. (2000) A double magmatic heat pump at the core–mantle boundary. *Am. Mineral.* **85,** 1589–1594.

Morse S. A. (2001a) Porous sediments at the top of the Earth's core? *Science* **291,** 2090–2091.

Morse S. A. (2001b) No mushy zones in the Earth's core. *J. Conference Abstr.* **6,** 426.

Morse S. A. and Allison J. P. (1986) Correlation between roof and floor cumulates of the Kiglapait intrusion, Labrador. *Geophys. Res. Lett.* **13,** 1466–1469.

Morse S. A., Owens B. E., and Butcher A. R. (1987) Origin of finger structures in the Rhum Complex: Phase equilibrium and heat effects. *Geol. Mag.* **124,** 205–210.

Poirier J.-P., Goddat A., and Peyronneau J. (1996) Ferric iron dependence on the electrical conductivity of the Earth's lower mantle material. *Phil. Trans. R. Soc. Lond. Ser. A* **354,** 1361–1369.

Poirier J.-P., Malavergne V., and Le Mouël J. L. (1998) Is there a thin electrically conducting layer at the base of the mantle? In *The Core–Mantle Boundary Region* (eds. M. Gurnis, et al.), pp. 131–137 AGU Geodynamics Series 28.

Presnall D. C. (1995) Phase diagrams of Earth-forming minerals (ed. T. J. Ahrens), In *Mineral Physics and Crystallography, 2,* 248–268 AGU Reference Shelf.

Rost S. and Revenaugh J. (2001) Seismic detection of rigid zones at the top of the core. *Science* **294,** 1911–1914.

Rushmer T., Minarik W. G., and Taylor G. J. (2000) Physical processes of core formation. In *Origin of the Earth and Moon* (eds. R. M. Canup and K. Righter), 227–243. Univ. Arizona Press: Tucson.

Secco R. A. (1995) Viscosity of the outer core (ed. T. J. Ahrens), In *Mineral Physics and Crystallography, 2,* 218–226 AGU Reference Shelf.

Selkin P. A., Gee J. S., and Meurer W. P. (2000) Late Archean paleointensity from the Stillwater Complex, MT (Abs.). *EOS Trans. AGU* **81,** F365.

Sporleder B. A. (1998) Liquid line of descent of the Lower Zone of the Kiglapait intrusion, Labrador, Canada: An experimental study. M.S. thesis, University of Massachusetts.

Stacey F. D. (1992) *Physics of the Earth*. Brookfield Press.

Stevenson D. J. (1981) Models of the Earth's core. *Science* **214,** 611–619.

Stevenson D. J. (1986) Mercury's magnetic field revisited: A new model. *Lunar Planet. Sci.* **17,** 1009–1010.

Turcotte D. L. and Schubert G. (1982) *Geodynamics*. Wiley: New York.

Turner J. S. (1965) The coupled turbulent transports of salt and heat across a sharp density interface. *Int. J. Heat Mass Transfer* **8,** 759–67.

Wager L. R., Brown G. M., and Wadsworth W. J. (1960) Types of igneous cumulates. *J. Petrol.* **1,** 73–85.

Wasson J. T. (1974) *Meteorites: Classification and Properties*. Springer-Verlag.

Williams Q. (1998) The temperature contrast across D″. In *The Core–Mantle Boundary Region* (eds. M. Gurnis, et al.), pp. 73–82 Series 28. AGU Geodynamics.

Williams Q. and Garnero E. J. (1996) Seismic evidence for partial melt at the base of the Earth's mantle. *Science* **273,** 1528–1530.

Wood B. J. and Nell J. (1991) High-temperature electrical conductivity of the lower-mantle phase. *Nature* **351,** 309–311.

Yamazaki D. and Karato S.-I. (2001) Some mineral physics constraints on the rheology and geothermal structure of Earth's lower mantle. *Am. Mineral.* **86,** 385–391.